



# Influence of $\text{NH}_4\text{Br}$ as an ionic source on the structural/electrical properties of dextran-based biopolymer electrolytes and EDLC application

M H HAMSAN<sup>1</sup>, M F SHUKUR<sup>2</sup>, SHUJAHADEN B AZIZ<sup>3,4</sup>, Y M YUSOF<sup>5</sup> and M F Z KADIR<sup>6,\*</sup> 

<sup>1</sup>Institute for Advanced Studies, University of Malaya, 50603 Kuala Lumpur, Malaysia

<sup>2</sup>Fundamental and Applied Sciences Department, Universiti Teknologi PETRONAS, 32610 Seri Iskandar, Malaysia

<sup>3</sup>Advanced Polymeric Materials Research Laboratory, Department of Physics, College of Science, University of Sulaimani, Sulaimani, Kurdistan Regional Government 46001, Iraq

<sup>4</sup>Komar Research Center (KRC), Komar University of Science and Technology, Sulaimani, Kurdistan Regional Government 46001, Iraq

<sup>5</sup>Universiti Kuala Lumpur Malaysian Institute of Chemical and Bio-Engineering Technology (UniKL MICET), 78000 Alor Gajah, Malaysia

<sup>6</sup>Centre for Foundation Studies in Science, University of Malaya, 50603 Kuala Lumpur, Malaysia

\*Author for correspondence (mfzkadir@um.edu.my)

MS received 22 May 2019; accepted 20 August 2019

**Abstract.** Biopolymer electrolytes (BPEs), consisting of ammonium bromide ( $\text{NH}_4\text{Br}$ ) as the ionic provider and dextran (*Leuconostoc mesenteroides*) as the polymer host, are prepared by the solution cast technique. Interactions of cations from the salt have been confirmed with hydroxyl (OH) and glycosidic linkage (C–O–C) groups of dextran *via* Fourier transform infrared analysis. Electrolyte with 20 wt%  $\text{NH}_4\text{Br}$  maximized the ionic conductivity up to  $(1.67 \pm 0.36) \times 10^{-6} \text{ S cm}^{-1}$ . The trend of conductivity has been verified by field emission scanning electron microscopy, where the electrolyte surface became rough as the concentration of  $\text{NH}_4\text{Br}$  exceeded 20 wt%. The contribution of ions as the main charge carrier in the BPE is confirmed by transference number analysis as  $t_{\text{ion}} = 0.92$  and  $t_{\text{e}} = 0.08$ . From linear sweep voltammetry, it is found that the highest conducting BPE in this work is electrochemically stable from 0 to 1.62 V. The fabricated electrochemical double-layer capacitor (EDLC) has been tested for 100 charge–discharge cycles and verified by cyclic voltammetry.

**Keywords.** Ammonium bromide; dextran; polymer electrolyte; ionic conductivity; biopolymer.

## 1. Introduction

Biopolymers, e.g. dextran, pectin, starch, carrageenan, cellulose, chitosan and algae, have been studied as the electrodes separator in energy storage devices such as solar cells, electrochemical double-layer capacitors (EDLCs), batteries and fuel cells by many researchers [1–3]. This is due to increasing demand on electrical devices such as laptops, tablets, televisions and phones. This demand indirectly increases the waste from electrical devices. According to Orlins and Guan [4], the second highest electrical waste source is mobile phones. Hence, the use of electrolyte based on biodegradable biopolymers can reduce the amount of electrical waste.

Typical polysaccharides possess oxygen containing functional groups attached to their polymer backbones. This oxygen atom possesses lone pair electrons which form dative bond with cation from the salt for the conduction process [5]. Unique characteristic of biopolymer such as good film forming, ionic conductor, easy preparation, inexpensive

as well as abundance makes them suitable for polymer host in electrolyte application [6]. Dextran is extracted from bacteria (*Leuconostoc mesenteroides*) culturing process in an environment of sucrose. Dextranase enzyme from the medium is then converted to dextran [7]. The structure of dextran consists of 1,6- $\alpha$ -D-glucopyranosidic, which is bonded by glycosidic linkages [8].

Common ionic sources for polymer electrolyte studies are sodium, lithium, silver and ammonium salt. Some alkali metals e.g. lithium and sodium salts are reactive with the presence of water molecules as well as thermally unstable [9]. Limitation of solvent for inorganic salts like potassium iodide (KI) and sodium iodide (NaI) makes them less preferable to be used as ionic dopant [10]. Ammonium salts can be employed to avoid the use of expensive and harmful lithium metal electrode in lithium batteries application. High ionic conductivity of biopolymer electrolyte (BPE) based on ammonium salt has been verified by many researchers [11,12].

Current advance made in portable electronics and the developing trend towards device miniaturization has attracted

researchers to study more on the EDLC. EDLC is a substitute for conventional batteries. The energy storage for EDLC is non-Faradaic reaction where ions form a double-layer on the carbon-based electrodes [13]. Activated carbon has been discovered to be compatible with polymer electrolyte. Activated carbon possesses unique characteristics, e.g. inexpensive, good chemical stability and high electrical conductivity as well as large surface area makes it preferable to be used in EDLC [14,15]. Structural and electrical tests have been done in this work for dextran–ammonium bromide ( $\text{NH}_4\text{Br}$ ) system, where dextran is the polymeric network for ions from  $\text{NH}_4\text{Br}$  conduct. The highest conducting electrolyte will be used as electrodes separator in the EDLC. This study enhances the knowledge regarding renewable green technology.

## 2. Methods and procedures

### 2.1 Preparation of BPE

Acetic acid (1%, 50 ml) was used to dissolve 2 g of dextran powder (Sigma-Aldrich, average molecular weight = 35000–45000) for ~40 min. Various amounts of  $\text{NH}_4\text{Br}$ , i.e. 5, 10, 15, 20, 25 and 30 wt% (Bendosen,  $M = 97.94 \text{ g mol}^{-1}$ ) were added to the dissolved dextran solution. The solutions were dried in different plastic Petri dishes at room temperature and room humidity of 50%. Before further analysis, BPE films were kept in desiccators.

### 2.2 BPE characterizations

The complexation between  $\text{NH}_4\text{Br}$  and dextran polymer was analysed via Fourier transform infrared (FTIR) spectroscopy using a Spotlight 400 Perkin-Elmer spectrometer. The resolution used was  $1 \text{ cm}^{-1}$  in the band region of 1120–1190 and 3000–3600  $\text{cm}^{-1}$ . A Hitachi SU8220 was employed to conduct field emission scanning electron microscopy (FESEM) at  $2\text{k}\times$  magnification. The ionic conductivity of BPE was obtained via electrical impedance spectroscopy (EIS) using a HIOKI 3532-50 LCR HiTESTER. The frequency range was from 50 Hz to 5 MHz. The BPE film was sandwiched to stainless steel (SS) of a teflon holder. The bulk resistance ( $R_{\text{bulk}}$ ) of the BPE was extracted from the Nyquist plots. The conductivity value was calculated as:

$$\sigma = \frac{t}{R_{\text{bulk}}A}. \quad (1)$$

Here,  $A$  is SS–BPE contact area and  $t$  is the thickness of BPE.

A V&A Instrument DP3003 digital DC power supply was used to analyse the ionic ( $t_{\text{ion}}$ ) and electronic ( $t_{\text{elec}}$ ) transference number (TNM) at 0.20 V. The electrochemical stability of BPE was verified by linear sweep voltammetry (LSV) using a Digi-IVY DY2300 potentiostat at  $100 \text{ mV s}^{-1}$ . The cell arrangement for TNM and LSV is the same as that for EIS analysis.

### 2.3 EDLC fabrication and characterization

Carbon black (0.25 g) was mixed with 3.25 g activated carbon in a planetary ball miller before the mixture was poured into a solution of 0.50 g of polyvinylidene fluoride (PVdF) and 15 ml N-methyl pyrrolidone (NMP). The solution was coated on the foil using a doctor blade. The electrodes were left in an oven to dry out at  $60^\circ\text{C}$ . The dried electrodes were placed in a desiccator for further drying. The electrode was cut into a small circle with area of  $2.01 \text{ cm}^2$ . Electrolyte with the highest conductivity was placed between two activated carbon electrodes and packed in a CR2032 coin cell. The EDLC characteristic was verified by cyclic voltammetry (CV) analysis at  $50 \text{ mV s}^{-1}$ . The EDLC charge–discharge profiles were tested using a Neware battery cycler with current density of  $0.063 \text{ mA cm}^{-2}$ . Specific capacitance ( $C_s$ ) can be calculated from CV curve as:

$$C_s = \frac{\int_{V_i}^{V_f} I(V) dV}{2mv(V_f - V_i)} \quad (2)$$

where  $I(V)dV$  is the area of the CV curve, which was determined using Origin 9.0 software;  $m$  and  $v$  are the mass of active material and scan rate, respectively.  $V_f$  and  $V_i$  in this work are 0.85 and 0 V, respectively.  $C_s$  from charge–discharge part and equivalent series resistance (ESR) were calculated using the given equations:

$$C_s = \frac{i}{ms}, \quad (3)$$

$$\text{ESR} = \frac{V_{\text{drop}}}{i}. \quad (4)$$

Here  $I$ ,  $s$  and  $V_{\text{drop}}$  are the applied current, slope of discharge part and voltage drop, respectively.

## 3. Results

Hydroxyl (OH) FTIR spectra for dextran– $\text{NH}_4\text{Br}$  BPE are shown in figure 1a. It is noticeable that OH peak for pure dextran film is at  $3398 \text{ cm}^{-1}$ . This result is comparable to those of other dextran studies [7,16,17]. OH peak is observed to shift to a lower wavenumber of  $3278 \text{ cm}^{-1}$  as 10 wt%  $\text{NH}_4\text{Br}$  is added. As 20 wt%  $\text{NH}_4\text{Br}$  was added, the peak shifted to  $3268 \text{ cm}^{-1}$ . The changes in OH's peak position signify the formation of dative bond between OH group of dextran and cation from the salt [18]. OH peak shifted back to a higher wavenumber of  $3273 \text{ cm}^{-1}$  as the concentration of  $\text{NH}_4\text{Br}$  exceeded 20 wt%. This indicates less interaction in OH region at this salt concentration [19]. FTIR spectra of glycosidic linkage (C–O–C) band region are portrayed in figure 1b, where for pure dextran it is centred at  $1153 \text{ cm}^{-1}$ . According to Azmeera *et al* [20] C–O–C peak for dextran is located at

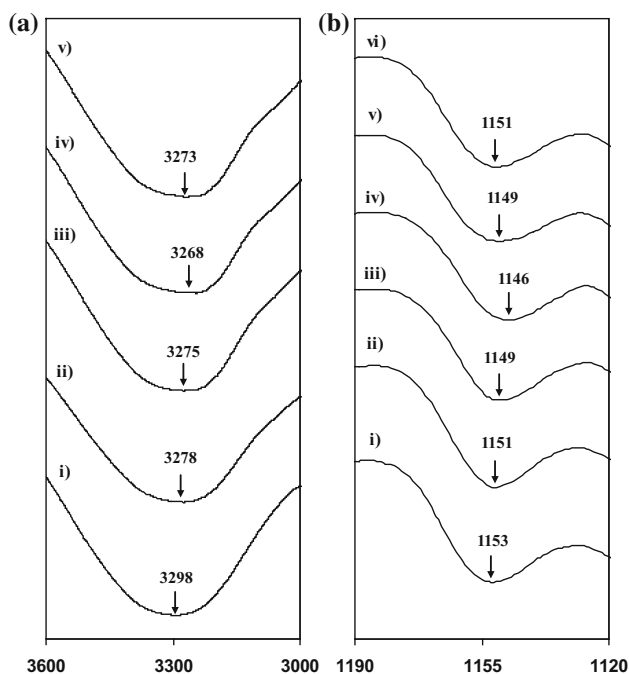


**Figure 1.** FTIR plot of electrolyte at (a) 3000–3600  $\text{cm}^{-1}$  and (b) 1120–1190  $\text{cm}^{-1}$  with (i) 0 wt%  $\text{NH}_4\text{Br}$ , (ii) 10 wt%  $\text{NH}_4\text{Br}$ , (iii) 15 wt%  $\text{NH}_4\text{Br}$ , (iv) 20 wt%  $\text{NH}_4\text{Br}$ , (v) 25 wt%  $\text{NH}_4\text{Br}$  and (vi) 30 wt%  $\text{NH}_4\text{Br}$ .

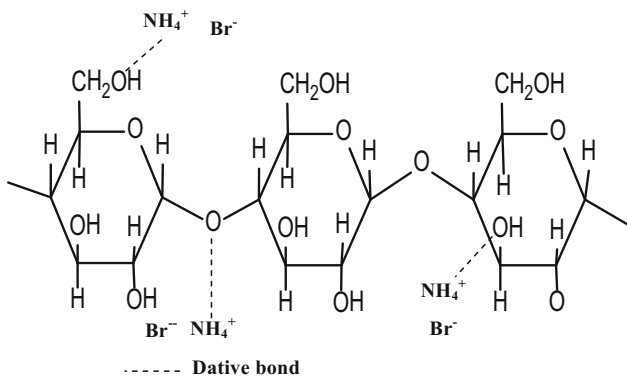


**Figure 2.** Possible interaction between dextran and  $\text{NH}_4\text{Br}$ .

1157  $\text{cm}^{-1}$ , which is almost similar in this study. C–O–C peak is observed at 1146  $\text{cm}^{-1}$  when 20 wt%  $\text{NH}_4\text{Br}$  is included. As more salt is added, more ions are available to interact with lone pair electron at oxygen of C–O–C groups [21]. When 25 and 30 wt%  $\text{NH}_4\text{Br}$  are added, the peak is observed to shift back to higher wavenumber. This implies the development of ion aggregations that reduce the concentration of charge carrier, thus reducing the ionic conductivity [22]. The possible interactions between cations from  $\text{NH}_4\text{Br}$  and the functional groups of dextran through dative bond are shown in figure 2.

**Table 1.** Room temperature conductivity of dextran BPE at various concentrations of  $\text{NH}_4\text{Br}$ .

$\text{NH}_4\text{Br}$ content (wt%)	Conductivity ( $\text{S cm}^{-1}$ )
0	$(8.24 \pm 3.13) \times 10^{-11}$
5	$(1.33 \pm 0.48) \times 10^{-10}$
10	$(3.25 \pm 0.84) \times 10^{-9}$
15	$(3.98 \pm 1.74) \times 10^{-7}$
20	$(1.67 \pm 0.36) \times 10^{-6}$
25	$(7.04 \pm 0.92) \times 10^{-7}$
30	$(2.77 \pm 7.78) \times 10^{-8}$

### 3.1 Ionic conductivity of BPE at room temperature

The conductivity of dextran– $\text{NH}_4\text{Br}$  BPE at room temperature is listed in table 1. Dextran film has ionic conductivity of  $(8.24 \pm 3.13) \times 10^{-11} \text{ S cm}^{-1}$ . The conductivity is then increased to  $(3.25 \pm 0.84) \times 10^{-9}$  and  $(1.67 \pm 0.36) \times 10^{-6} \text{ S cm}^{-1}$  with 10 and 20 wt%  $\text{NH}_4\text{Br}$ , respectively. From 5 to 20 wt%  $\text{NH}_4\text{Br}$ , the conductivity increases due to improvement of polymer segmental motion and charge carriers mobility [23]. As reported in our previous paper [17], dextran host doped with 20 wt% ammonium nitrate ( $\text{NH}_4\text{NO}_3$ ) BPE maximized a conductivity value of  $(3.00 \pm 1.60) \times 10^{-5} \text{ S cm}^{-1}$  at room temperature.  $\text{NH}_4\text{NO}_3$  is expected to provide more ions and higher conductivity value compared with  $\text{NH}_4\text{Br}$ . This is due to lower lattice energy of  $\text{NH}_4\text{NO}_3$  (648.9  $\text{kJ mol}^{-1}$ ) compared with  $\text{NH}_4\text{Br}$  (682.0  $\text{kJ mol}^{-1}$ ). Low lattice energy indicates easier ion dissociation process, thus resulting in higher conductivity value [24]. This pattern is harmonized with FTIR result, where the OH and C–O–C peaks shifted to lower wavenumber upon the addition of 20 wt%  $\text{NH}_4\text{Br}$ . At concentration of 25 and 30 wt%, the conductivity is observed to decrease. This is because at higher salt concentration, the polymer matrix can no longer accommodate excess ions, which leads to the development of ion pair, triplets and aggregations. This phenomenon decreases the ionic mobility and number density, which reduces the ionic conductivity of the BPE [25]. From FTIR analysis, OH and C–O–C peaks have shifted to higher wavenumber for BPE with 25 and 30 wt%  $\text{NH}_4\text{Br}$ .

### 3.2 Observation of BPE surface via FESEM study

The changes of the BPE surface at various concentrations of  $\text{NH}_4\text{Br}$  are shown in figure 3. Based on figure 3a, dextran film has a clear and smooth surface, which is comparable to our previous report [17]. As 10 wt%  $\text{NH}_4\text{Br}$  is added, the surface of the electrolyte possesses uniformly dispersed grains. More grains can be observed when 15 wt%  $\text{NH}_4\text{Br}$  is doped into the dextran film. These uniform grains are considered to be ion traps in the polymer matrix of dextran [26]. The presence of grains is still noticeable in figure 3d, as 20 wt%



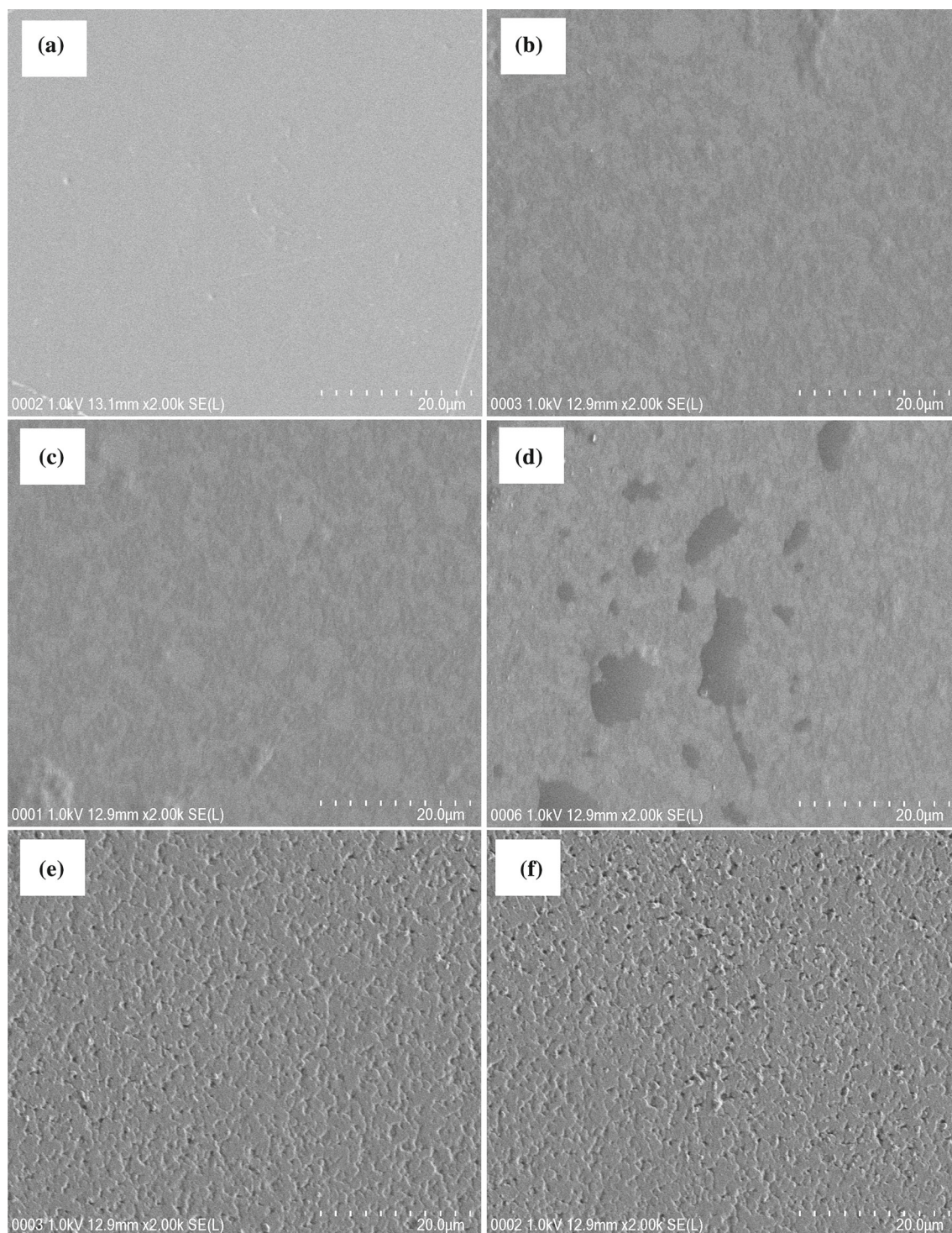


**Figure 3.** Surface FESEM image of electrolyte with (a) 0 wt%  $\text{NH}_4\text{Br}$  (pure dextran film), (b) 10 wt%  $\text{NH}_4\text{Br}$ , (c) 15 wt%  $\text{NH}_4\text{Br}$ , (d) 20 wt%  $\text{NH}_4\text{Br}$ , (e) 25 wt%  $\text{NH}_4\text{Br}$  and (f) 30 wt%  $\text{NH}_4\text{Br}$ .

$\text{NH}_4\text{Br}$  is added with a few dark spots. It has been reported that these dark areas indicate amorphous regions [27,28]. This result is consistent with the trend of conductivity where the electrolyte with 20 wt%  $\text{NH}_4\text{Br}$  has the highest conductivity

value. Surface of BPE becomes rough as the concentration of  $\text{NH}_4\text{Br}$  goes beyond 20 wt%  $\text{NH}_4\text{Br}$ . This signifies the recombination of ions and recrystallization of salt, which reduce the free ions [29]. This condition decreases the ionic conductivity.

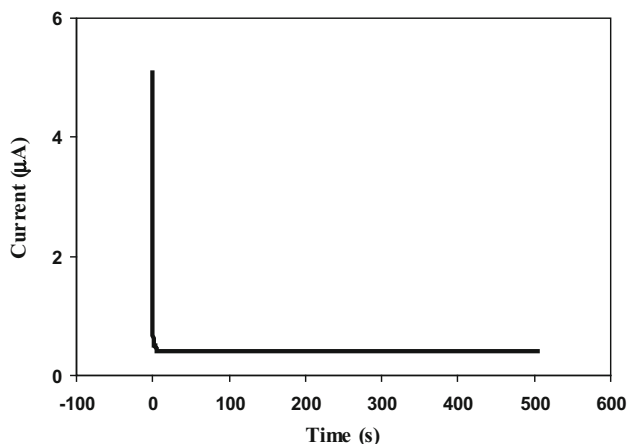


**Figure 4.** TNM plot of dextran-NH<sub>4</sub>Br BPE at 0.20 V.

### 3.3 TNM determination

The involvement of ions and electrons in the total conductivity can be determined by TNM analysis. Figure 4 shows the polarization of SS|20 wt% NH<sub>4</sub>Br|SS vs. time at working voltage of 0.20 V;  $t_{\text{ion}}$  and  $t_{\text{elec}}$  can be obtained from the following equations [30]:

$$t_{\text{elec}} = I_s / I_i \quad (5)$$

$$t_{\text{ion}} = 1 - t_{\text{elec}} \quad (6)$$

where  $I_i$  is the initial current and  $I_s$  is steady-state current. From figure 4,  $I_s$  and  $I_i$  are observed to be 0.4 and 5.1  $\mu\text{A}$ , respectively. Hence,  $t_{\text{ion}}$  and  $t_{\text{elec}}$  of dextran-NH<sub>4</sub>Br BPE are 0.92 and 0.08, respectively. Shukur and Kadir [31] reported  $t_{\text{ion}}$  and  $t_{\text{elec}}$  of 0.91 and 0.09, respectively, for starch-chitosan-NH<sub>4</sub>Cl system. Current is observed to reduce sharply initially. This is due to blocking effect of SS electrode; only electrons can pass through. Cations and anions in the BPE are polarized as a constant current (0.4  $\mu\text{A}$ ) is achieved [32].

### 3.4 Electrochemical stability test via LSV

The electrochemical stability is studied on the highest conducting dextran-NH<sub>4</sub>Br BPE by LSV analysis. The LSV curve of the BPE is depicted in figure 5. The voltage has been swept linearly up to 2.50 V until a large current is observed at a certain potential. This is attributed to the decomposition of BPE at the inert electrode interface [33]. Dextran-NH<sub>4</sub>Br BPE is electrochemically stable up to 1.62 V. This threshold voltage is in a sufficient range for the application in proton-based energy devices.

### 3.5 EDLC

CV analysis is conducted in EDLC studies to prove the capacitive behaviour of an EDLC. A scan rate of 50  $\text{mV s}^{-1}$

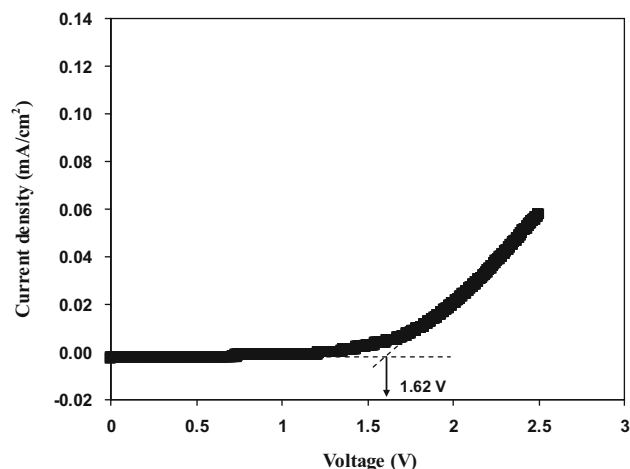


**Figure 5.** LSV curve of dextran-NH<sub>4</sub>Br BPE at a scan rate of 100  $\text{mV s}^{-1}$ .

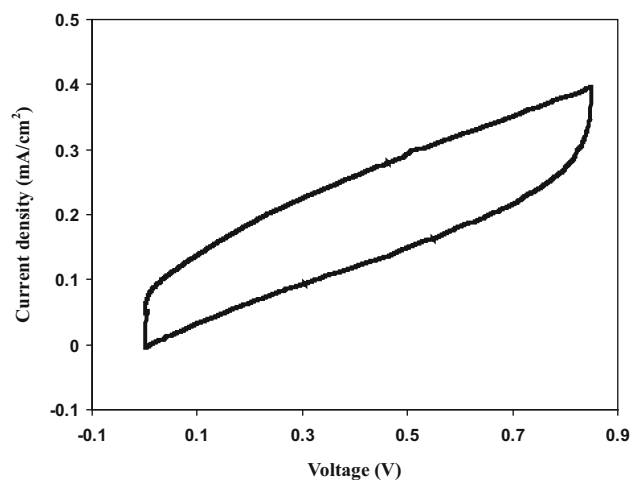
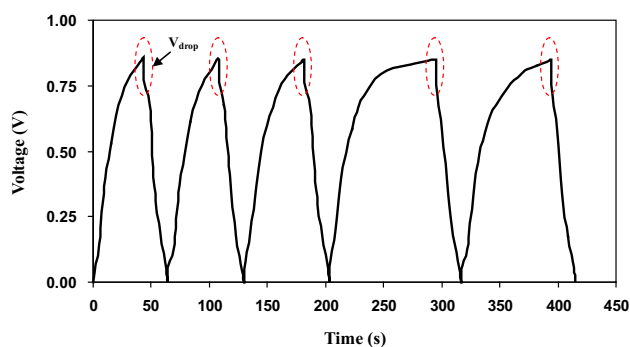


**Figure 6.** CV curve of the fabricated EDLC at 50  $\text{mV s}^{-1}$ .

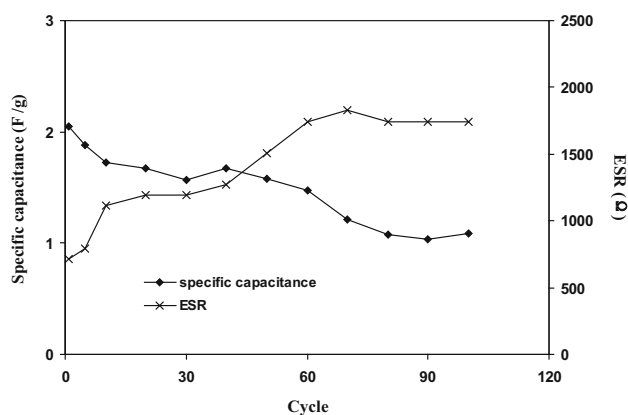
is applied for this analysis. CV plot of the fabricated EDLC can be seen in figure 6. No peaks are observed in the CV curve, signifying that neither oxidation nor reduction happens in the EDLC. This condition clearly shows the development of a charge double-layer at the surface of the carbon electrodes [34]. A perfect capacitor possesses a perfect rectangular CV curve. Due to internal resistance and porosity of the carbon electrodes, the shape of CV curve in this work is not completely a perfect rectangular shape [35].  $C_s$  of the EDLC has been calculated using the CV curve and equation (2). From CV,  $C_s$  is found to be 2.46  $\text{F g}^{-1}$ . This value will be compared to the one obtained in the charge-discharge curve.

Figure 7 shows the typical charge-discharge curve for the EDLC at selected cycles. It is noticeable that the discharge part is almost linear. This signifies that the fabricated EDLC has the capacitive characteristic [36]. The value of  $C_s$  is calculated using equation (3), which can be observed in figure 8.  $C_s$  at the 1<sup>st</sup> cycle is 2.05  $\text{F g}^{-1}$ . This value is comparable to the one





**Figure 7.** Charge–discharge curve for the fabricated EDLC at selected cycles.



**Figure 8.** Specific capacitance and ESR of the EDLC for 100 cycles.

obtained from CV analysis. The value of  $C_s$  is almost constant with the average of  $1.61 \text{ F g}^{-1}$  from 10<sup>th</sup> to 60<sup>th</sup> cycle. The performance of the EDLC is observed to reduce to  $1.10 \text{ F g}^{-1}$  at the 100<sup>th</sup> cycle. The value of ESR has been obtained from equation (4). From figure 8, the value of ESR at the 1<sup>st</sup> cycle is  $714 \Omega$ . The value of ESR then increases to  $1746 \Omega$  at the 100<sup>th</sup> cycle. The existence of internal resistance in the EDLC is due to the current collector used, electrolyte and gap between current collector and the electrolyte [37]. This explains the reduction in the value of  $C_s$  throughout the 100<sup>th</sup> cycle. As the cycle number increases, the development of ion aggregation increases due to rapid charge–discharge process. This condition reduces the free ions accumulation at the surface of the electrodes, which in turn reduces the specific capacitance [34].

#### 4. Conclusion

Solution cast technique has been successfully employed for synthesis of dextran doped with  $\text{NH}_4\text{Br}$  BPE. The complexation among the materials in the BPE has been verified by the shifting of OH and C–O–C peaks *via* FTIR outcomes. The addition of 20 wt%  $\text{NH}_4\text{Br}$  into dextran host has enhanced the ionic conductivity from  $\sim 10^{-11}$  to  $\sim 10^{-6} \text{ S cm}^{-1}$ . The trend of conductivity is further confirmed by studying the

changes of BPE surface *via* FESEM study. Ions have been confirmed to be the dominant charge carrier as  $t_{\text{ion}} = 0.92$  and  $t_{\text{elec}} = 0.08$ . Dextran– $\text{NH}_4\text{Br}$  BPE is electrochemically stable from 0 to 1.62 V as obtained from LSV analysis. The fabricated EDLC has been tested for 100 charge–discharge cycles with specific capacitance at 1<sup>st</sup> cycle =  $2.05 \text{ F g}^{-1}$ .

#### Acknowledgements

The authors thank University of Malaya for grant BKS005-2018 awarded and Universiti Kuala Lumpur (UniKL MICET) for FRGS/1/2018/STG07/UNIKL/02/8.

#### References

- [1] Shukur M F, Ithnin R and Kadir M F Z 2014 *Electrochim. Acta* **136** 204
- [2] Sampathkumar L, Christopher Selvin P, Selvasekarapandian S, Perumal P, Chitra R and Muthukrishnan M 2019 *Ionics* **25** 1067
- [3] Moniha V, Alagar M, Selvasekarapandian S, Sundaresan B, Hemalatha R and Boopathi G 2018 *J. Solid State Electrochem.* **2** 3209
- [4] Orlins S and Guan D 2016 *J. Clean. Prod.* **114** 71
- [5] Hamsan M H, Shukur M F and Kadir M F Z 2017 *Ionics* **23** 1137
- [6] Chai M N and Isa M I N 2016 *Sci. Rep.* **6** 1
- [7] Maria D, Madalina A, Marian V, Catalin V and Viorica M 2012 *Solid State Phenom.* **188** 102
- [8] Telegeev G, Kutsevol N, Chumachenko V, Naumenko A, Telegeeva P, Filipchenko S *et al* 2017 *Int. J. Polym. Sci.* **2017** 1
- [9] Osman Z, Mohd Ghazali M I, Othman L and Md Isa K B 2012 *Results Phys.* **2** 1
- [10] Kang J, Li W, Wang X, Lin Y, Li X, Xiao X *et al* 2004 *J. Appl. Electrochem.* **34** 301
- [11] Amran N N A, Manan N S A and Kadir M F Z 2016 *Ionics* **22** 1647
- [12] Hamsan M H, Shukur M F and Kadir M F Z 2017 *Ionics* **23** 3429
- [13] Hassan M F, Azimi M S N, Kamarudin K H and Sheng C K 2018 *ASM Sci. J.* **1** 17 (Special Issue)
- [14] Kamarudin K H, Hassan M and Isa M I N 2018 *ASM Sci. J.* **1** 29
- [15] Hezhen Y, Ying L, Lingbin K, Long K and Fen R 2019 *J. Power Sources* **426** 47
- [16] Mohanasrinivasan V, Ghosa T, Thaslim J B, Zeba H J, Selvarajan E, Suganthi V *et al* 2014 *Res. J. Pharm. Technol.* **7** 8
- [17] Hamsan M H, Shukur M F, Aziz S B and Kadir M F Z 2019 *Bull. Mater. Sci.* **42** 57
- [18] Salleh N S, Aziz S B, Aspanut Z and Kadir M F Z 2016 *Ionics* **22** 2157
- [19] Kadir M F Z, Aspanut Z, Majid S R and Arof A K 2011 *Spectrochim. Acta A* **78** 1068
- [20] Azmeera V, Adhikary P and Krishnamoorthi S 2012 *Int. J. Carbohydr. Chem.* **2012** 1
- [21] Hafiza M N and Isa M I N 2017 *Carbohydr. Polym.* **165** 123

- [22] Monisha S, Mathavan T, Selvasekarapandian S, Benial A, Aris-tatil G, Mani N *et al* 2017 *Carbohydr. Polym.* **157** 38
- [23] Kadir M F Z, Salleh N S, Hamsan M H, Aspanut N A and Shukur M F 2018 *Ionics* **24** 1651
- [24] Kadir M F Z 2010 *PhD thesis* (University of Malaya, Malaysia)
- [25] Misenan M S M, Isa M I N and Khair A S A 2018 *Mater. Res. Express* **2053** 1
- [26] Kadir M F Z, Majid S R and Arof A K 2010 *Electrochim. Acta* **55** 1475
- [27] Shukur M F 2015 *PhD thesis* (University of Malaya, Malaysia)
- [28] Su'ait R H Y, Ahmad A, Hamzah H and Rahman M Y A 2011 *Electrochim. Acta* **57** 123
- [29] Yusof Y M, Shukur M F, Illias H A and Kadir M F Z 2014 *Phys. Scr.* **89** 035701
- [30] Ramya C S and Selvasekarapandian S 2014 *Ionics* **20** 1681
- [31] Shukur M F and Kadir M F Z 2015 *Electrochim. Acta* **158** 152
- [32] Rani M S A, Ahmad A and Mohamed N S 2017 *Ionics* **24** 807
- [33] Tian K L, Ataollahi N, Hassan N H and Ahmad A 2016 *J. Solid State Electrochem.* **20** 203
- [34] Shuhaimi N E A, Teo L P, Woo H J, Majid S R and Arof A K 2012 *Polym. Bull.* **69** 807
- [35] Kadir M F Z and Arof A K 2013 *Mater. Res. Innov.* **15** 217
- [36] Teoh K H, Liew C W and Ramesh S 2014 *Ionics* **20** 251
- [37] Arof A K, Kufian M Z, Syukur M F, Aziz M F, Abdelrahman A E and Majid S R 2012 *Electrochim. Acta* **74** 39